Design of Line/Motor Side Capacitors for PWM CSR-CSI Drives to Achieve Optimal Power Factor in High Power Fan/Pump Applications

Y. Xiao and B.Wu   N. R. Zargari*   R. Sotudeh**

Dept. of Electrical and Computer Engineering
Ryerson Polytechnic University, Toronto, Canada M5B 2K3

*Allen-Bradley Canada
Cambridge, Canada N1R 5X1

**Dept. of Electronics and Computer Engineering
University of Teesside, Middlesbrough Cleveland, U.K. TS1 3BA

Abstract: The input power factor of GTO PWM current source rectifiers using a delay angle control scheme is investigated. It is discovered that with an optimal design of line and motor side capacitors for CSR-CSI induction motor drives having fan/pump loads, the input power factor is close to unity (over 0.95 for 30% to 100% of rated load). The concept of near unity power factor operation is presented. The procedures for the capacitor design are discussed. A switching pattern suitable for the delay angle control with a low harmonic distortion is also introduced. The line current of the rectifier is near sinusoidal due to the use of the switching pattern and line side capacitor. Experimental results on a 5hp drive are given to verify the theoretical analysis.

Fig. 1   Circuit diagram of GTO PWM current source rectifier

Fig. 2   A GTO CSR-CSI induction motor drive system

I Introduction

GTO current source inverter based induction motor drivers are often used in petrochemical industry, mining and metals industry, water pumping systems and utility plants to drive high power fans and pumps. In these applications, SCR rectifiers are usually used as a front end converter[1,2]. The SCR rectifier, however, produces harmonics into the power systems and its power factor is poor under light load conditions.

These problems can be solved by replacing the SCR rectifier with a GTO PWM current source rectifier (CSR) as shown in Fig. 1. A line side capacitor is required by the rectifier to provide a current path for the energy stored in the line reactor when a GTO device is turned off. The ac input current of the rectifier is modulated to eliminate certain harmonics while the dc output current is controlled by modulation index M_d [3,4].

In general, the GTO current source rectifier produces a leading power factor due to the line capacitor. To achieve unity or maximum power factor operation, a delay angle α between the rectifier input voltage and modulated current should be introduced to generate a lagging current component
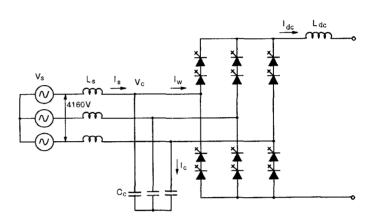
which compensates the leading current produced by the capacitor. Integrating the α control with modulation index M_d control makes the control scheme complicated. For example, both feedforward and feedback techniques should be used to implement the α plus M_d control scheme[5,6].

In this paper, the input power factor of the CSR using the delay angle control only is investigated. It is discovered that with an optimal design of line and motor side capacitors for the CSR-CSI induction motor drives having fan/pump loads (Fig. 2), the input power factor can be kept at least 0.95 over a normal drive operating range. Furthermore, the PWM rectifier using the α control scheme has the following additional features:

■   The switching frequency is only 300Hz, which is the

lowest switching frequency for 5th and 7th harmonic elimination. Therefore, the GTO and snubber losses are minimized;

■ The control for the PWM rectifier is simple and easy to implement. The modulation index control is no longer required; and

■ The total harmonic distortion generated by this switching pattern is much lower than that by other patterns. The use of this switching pattern and line side capacitor makes the line current near sinusoidal.

II Switching Pattern and Rectifier Control

One of the basic requirements for the switching pattern used in high power converters is that the switching frequency should be minimized to accommodate the GTO switching characteristic and to reduce GTO switching/snubber losses. A switching pattern suitable for the current source rectifier using delay angle control is proposed. A comparison between the delay angle α control and modulation index M_d control is given in Table 1. Obviously, the α control is superior to the M_d control because of its lower switching frequency, fixed switching angles and low harmonic distortion.

Table 1 Comparison of switching patterns between α and M_d controls

Control scheme		α control	M_d control
Switching frequency (Hz)		300	360
Switching angles		Fixed	Variable
Harmonic eliminated		5th & 7th	5th & 7th
Harmonic contents (%)	11th	23.3 (fixed)	56.3 (max.)
	13th	28.6	29.3
	17th	15.8	15.8
	19th	0.8	27.4

III Power Factor Analysis

The input power factor of the drive system is mainly determined by the line and motor side capacitors, the delay angle α and the load profile of the induction motor. For a fan and pump type of loads, the load torque and power are proportional to the second and third power of the motor speed. In the follows, a set of equations are derived to assist the analysis of input power factor of the drive system.

Motor Side Equations

Assuming that the air gap flux of the induction motor is kept constant during operation, neglecting the effect of stator resistance and leakage inductance, the air gap flux can be expressed as

$$\lambda_s = \frac{V_s'}{\omega_s} = 1 \qquad pu \qquad (1)$$

From which

$$V_s' = \omega_s \qquad (2)$$

where V_s' is the stator voltage and ω_s is the stator (operating) frequency, all in per unit.

For fan or pump applications, the torque is proportional to the speed square. Assuming at the rated speed, the torque is also rated, the torque-speed relationship can be described by

$$T = \omega_s^2 \qquad pu \qquad (3)$$

Neglecting all the losses in the drive system, the real power required from the inverter is

$$P = T_s \omega_s = \omega_s^3 \qquad pu \qquad (4)$$

from which the stator current can be calculated:

$$I_s' = \frac{P}{V_s'\cos\phi} = \frac{\omega_s^2}{\cos\phi} \qquad pu \qquad (5)$$

where ϕ is the power factor angle of the motor. The real and imaginary components of the stator current are

$$I_{s,r}' = I_s' \cos\phi = \omega_s^2 \qquad (6)$$

and

$$I_{s,x}' = I_s' \sin\phi = \omega_s^2 \tan\phi \qquad (7)$$

The capacitor current can be calculated by

$$I_c' = \omega_s C_i V_s' = \omega_s^2 C_i \qquad (8)$$

334

Thus, the inverter output current is

$$I_w' = \omega_s^2 \sqrt{1+(C_i-\tan\phi)^2} \qquad (9)$$

Line Side Equations

As mentioned earlier, a fixed PWM switching pattern is proposed for the rectifier to eliminate 5th and 7th while the dc link current I_d is controlled by the delay angle α. Therefore, the rectifier side modulation index, defined by

$$M_d = \frac{I_w}{I_d} \qquad (10)$$

is fixed. On the motor side, the inverter output current I_w' is proportional to the dc link current, whereas the use of the PWM technique is only for the harmonic elimination. Hence the inverter modulation index ($M_d' = I_w' / I_d$) can also be considered constant and equal to line side modulation index, which results in

$$I_w = I_w' = \omega^2 \sqrt{1+(C_i-\tan^{-1}\phi)^2} \qquad (11)$$

According to the rectifier phasor diagram shown in Fig. 3, the real (input) power of the rectifier is

$$P = V_s I_w \cos\alpha \qquad (12)$$

from which

$$\cos\alpha = \frac{P}{V_s I_w} = \frac{P}{I_w}$$
$$= \frac{\omega_s}{\sqrt{1-(C_i-\tan^{-1}\phi)^2}} \qquad (13)$$

where $V_s = 1.0\ pu$. Assuming the motor power factor is unity for simplicity, Eq. (13) can be rewritten as

$$\cos\alpha = \frac{\omega_s}{\sqrt{1+C_i^2}} \qquad (14)$$

From Eqs. (11) and (14), the real and imaginary components of I_w can be evaluated by
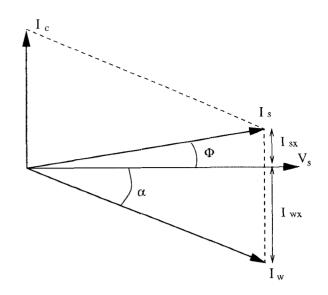
$$I_{w,r} = I_w \cos\alpha = \omega_s^3 \qquad (15)$$

Fig. 3   Phasor diagram of PWM current source rectifier

and

$$I_{w,x} = I_w \sin\alpha = I_w \sqrt{1-\cos^2\alpha}$$
$$= \omega_s^2 \sqrt{1+C_i^2-\omega_s^2} \qquad (16)$$

Finally, the reactive component of the source current can be calculated by

$$I_{s,x} = V_s \omega C_s - I_{w,x}$$
$$= C_c - \omega_s^2\sqrt{1+C_i^2-\omega_s^2}\ \ pu \qquad (17)$$

where ω is the frequency of source voltage, which is equal to 60Hz (1.0pu).

To achieve unity input power factor at motor rated operating point where $\omega_s \approx 1$, the reactive component given in Eq. (17) should be zero, from which the relationship between line and motor side capacitances can be obtained:

$$C_c = C_i \qquad (18)$$

It is very interesting to note that the reactive component of the line current does not change much over a certain operation range, which implies that the input power factor can be kept close to unity. For example, assuming that the drive is operated at 40% of the load with $C_c = C_i$ per unit, the reactive component is

$$I_{s,x} = 0.4 - 0.74^2\sqrt{0.4^2 + 1 - 0.74^2}$$

$$= 0.028 \; pu$$

(19)

and the corresponding input power factor is 0.997.

The concept of power factor control is further illustrated in Fig. 4, where the motor capacitor is 0.6 per unit and motor power factor is assumed to be unity. The input power factor varies with the line capacitor size and motor output power. The best power factor profile can be obtained when the line capacitor size is made equal to that of the motor capacitor.
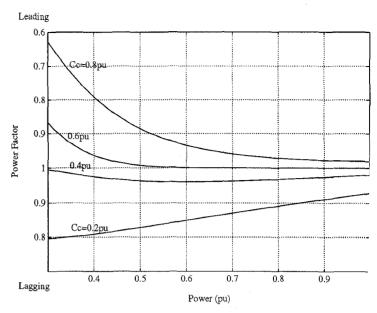
Figure 5 shows the input power factor profile where the system parameters remain the same as given in Fig. 4 except that the rated motor power factor is 0.9. A good input power factor profile can be obtained when a smaller size of the line capacitor is selected ($C_c = 0.4$ per unit in this case).
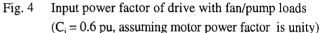
The design of the capacitors involves two steps. The first step is to determine the motor side capacitor. The size of this capacitor is mainly dependent on inverter switching frequency. For a drive system with a switching frequency of 180Hz, the capacitor value of 0.4 to 0.7pu will make the motor current and voltage waveforms nearly sinusoidal [1]. Considering the fact that the line capacitor should be smaller than motor capacitor to achieve a good power factor profile as shown in Fig. 5, a motor capacitor value close to its upper limit (0.6 to 0.7pu) can be selected such that the line capacitor size can be increased accordingly to improve the input current waveform.

The second step is to determine the line side capacitor. This could be accomplished graphically using a plot similar to Fig. 5, from which the line capacitor size can be selected.

IV Experimental Results

Table 2 shows some of the experimental results from a 208V, 5hp GTO current source induction motor drive with a fan type load of load. According to the design steps discussed above, a line capacitor of 0.4 can and motor capacitor of 0.67pu are selected. The input power factor of the drive with 100% and 30% of rated load is 0.96 (leading) and 0.98 (lagging), respectively. Since the line current is close to sinusoidal, distortion factor is neglected and only the displacement factor is considered here. Figure 6 illustrates the waveforms of the source voltage V_s, source current I_s and rectifier input current I_w with two different loadings. It can be seen that under the rated load condition, the system input power factor is leading. When the drive operates at 30% of the rated load, a slightly lagging power factor is observed.
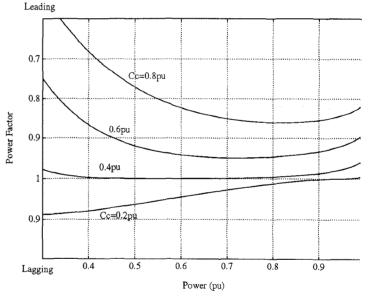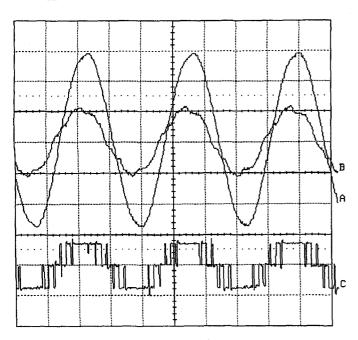

Fig. 4   Input power factor of drive with fan/pump loads
($C_i = 0.6$ pu, assuming motor power factor is unity)

Fig. 5   Input power factor of drive with fan/pump loads (C_i = 0.6 pu, motor rated power factor = 0.9)

V Conclusions

The input power factor of GTO PWM current source rectifiers using a delay angle control scheme is investigated. It is discovered that with an optimal design of line and motor side capacitors for CSR-CSI induction motor drives having fan/pump loads, the input power factor is close to unity (over 0.95 for 30% to 100% of rated load). The concept of near unity power factor operation is presented. The procedures for the capacitor design are discussed. A switching pattern suitable for the delay angle control with a low harmonic distortion is also introduced. The line current

Table 2 Experimental results from a 5hp induction motor drive system

P_{out} (pu)	0.31	0.43	0.64	0.79	1.0
ω_{motor} (pu)	0.68	0.76	0.86	0.93	1.0
PF_{motor}	0.57	0.60	0.72	0.75	0.79
PF_{input}	0.98 (lagging)	1.0	0.99 (leading)	0.99 (leading)	0.96 (leading)

(a) Rated load

(b) 30% of rated load

Trace A: Line-to-neutral voltage 50V/div
        B: Line current I_s 20A/div
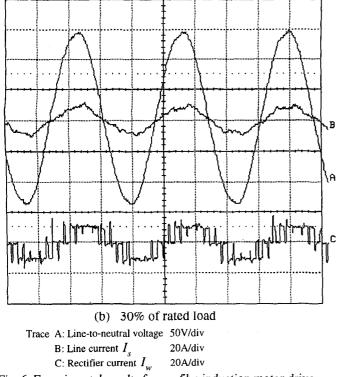   C: Rectifier current I_w 20A/div

Fig. 6 Experimental results from a 5hp induction motor drive

of the rectifier is near sinusoidal due to the use of the switching pattern and line side capacitor. Experimental results on a 5hp drive are given to verify the theoretical analysis.

Reference:

[1] B. Wu, S. A. Dewan and G. R. Slemin, "PWM-CSI inverter for induction motor drives," IEEE Trans. IA., 1992, pp64-71.

[2] P. M. Espelage, J. M. Nowak, " Symmetrical GTO current source inverter for wide speed range control of 2300 to 4160 volt, 350 tp 7000hp, induction motors," IEEE IAS Annual Meeting, pp302-307, 1988.

[3] M. Iwahori and K. Kousaka, " Three-phase current source rectifier adopting new PWM control techniques," IEEE IAS Annual Meeting, 1989, pp.855-860.

[4] H. R. Karshenas, H. A. Kojori and S.B. Dewan, "Generalized techniques of selective harmonic elimination in rurrent source inverters/converters," IEEE Trans. IA., 1995, pp566-573.

[5] J.H. Choi, H.A. Kojori, and S.B. Dwan, " High power GTO-CSC based power supply utilizing SHE-PWM and operating at unity power factor," CCECE, 1993.

[6] Y. Xiao, B. Wu, S. Rizzo and R. Sotudeh, "A novel power factor control scheme for high power GTO current source converter," IEEE IAS Annual Meeting, 1996 (to be published).